Source terms for calculations of vaporizing and burning fuel sprays with non-unity Lewis numbers in gases with temperature-dependent thermal conductivities

By J. Urzay, H. Pitsch AND A. Liñán

1. Motivation and objectives

Liquid-fueled burners are used in a number of propulsion devices ranging from internal combustion engines to gas turbines. The structure of spray flames is quite complex and involves a wide range of time and spatial scales in both premixed and non-premixed modes (Williams 1965; Luo *et al.* 2011). A number of spray-combustion regimes can be observed experimentally in canonical scenarios of practical relevance such as counterflow diffusion flames (Li 1997), as sketched in figure 1, and for which different microscale-modelling strategies are needed. In this study, source terms for the conservation equations are calculated for heating, vaporizing and burning sprays in the single-droplet combustion regime. The present analysis provides extended formulation for source terms, which include non-unity Lewis numbers and variable thermal conductivities.

2. Derivation of the droplet heating, vaporization and burning-rate formulae for gaseous atmospheres with temperature-dependent thermal conductivity and non-unity Lewis numbers

Consider a spherical fuel droplet of radius a and density ρ_d surrounded by a gas with density ρ. The fuel droplet can be heated by the surrounding gas and become vaporized, with the resulting fuel vapor F reacting with the ambient oxidizer O_2 according to the irreversible one-step Arrhenius reaction $F + sO_2 \rightarrow (1+s)P + q$, where P is the product, q is the chemical heat released, and s is the mass of oxidizer reacting with the unit mass of fuel in stoichiometric proportions. A local stoichiometric factor $S_L = s/Y_{O_2}$ is defined, which is based on the surrounding oxidizer mass fraction Y_{O_2}. For sufficiently large liquid-gas density ratios $\rho_d/\rho \gg 1$, with $\rho_d/\rho \sim 10^2 - 10^3$ for typical fuels and combustor pressures, the characteristic vaporization time $(\rho_d/\rho)(a^2/D_T)$ is much longer than the diffusion time a^2/D_T and the vaporization process can be considered to occur quasi-steadily, with $v_c = (\rho_d/\rho)|da/dt| \gg |da/dt|$ the gas velocity at the droplet surface. Similarly, if the droplet moves sufficiently slowly, the mechanical time $a/|\mathbf{v} - \mathbf{v}_d|$ is much longer than the diffusion time a^2/D_T, or equivalently, the Péclet number is small, $\mathrm{Pe}_d = |\mathbf{v} - \mathbf{v}_d|a/D_T \ll 1$, where $\mathbf{v}$ and $\mathbf{v_d}$ are, respectively, the gas and droplet velocity vectors, and convection effects can be neglected up to distances of order a/Pe_d from the droplet surface. Additionally, if the spatial variations of the temperature and species concentrations in the gas are sufficiently small, the unsteady effects induced by the far field can be neglected for analyzing the vaporization process; for the mixing-layer problem of figure 1, this approximation requires that $\delta_M/|\mathbf{v}_d| \gg a^2/D_T$, with δ_M the mixing-layer thickness. When these conditions are satisfied, the heating and vaporization processes are

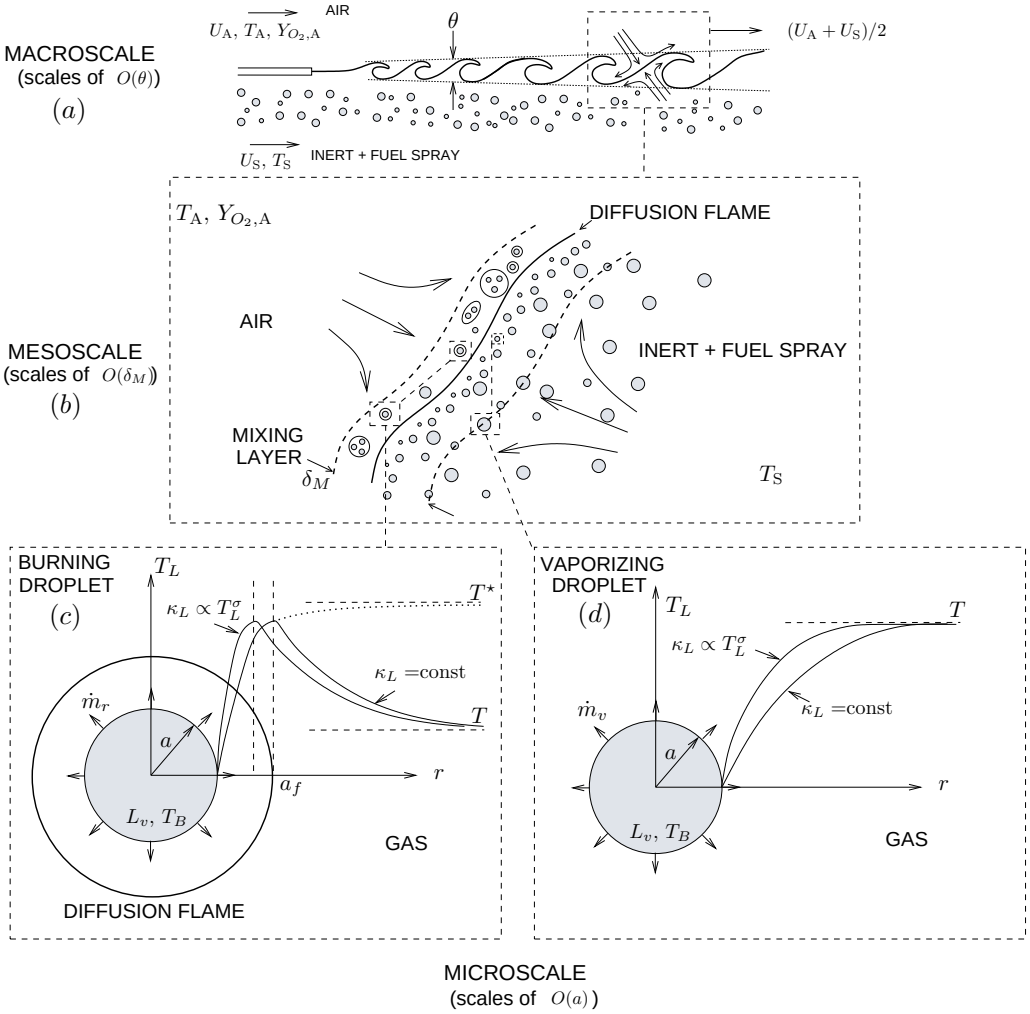

FIGURE 1. Separation of scales in a model mixing-layer problem with fuel-spray and oxidizer feed streams. (a) The mixing-layer problem viewed in scales of the same order as the momentum thickness θ. (b) A counterflow mixing layer of thickness δ_M is abstracted from a braid moving with the average velocity of the spanwise vortices. (c) Droplet burning and (d) droplet vaporization. The remaining symbols are defined in the main text.

spherically symmetric. Furthermore, if $\mathrm{Pe}_d \ll 1/S_L \ll 1$, the shape of the reaction zone is spherically symmetric, and the radial variation of the temperature around each droplet can be determined by integration of the energy equation

$$\frac{\dot m}{4\pi r^2}\frac{\mathrm{d}T_L}{\mathrm{d}r} = \frac{1}{r^2}\frac{\mathrm{d}}{\mathrm{d}r}\left(\rho_L D_{T,L} r^2 \frac{\mathrm{d}T_L}{\mathrm{d}r}\right) + \frac{q\omega_F}{c_p}, \tag{2.1}$$

where ω_F is the mass of fuel consumed per unit time and per unit volume, and $\dot m = 4\pi\rho v_c r^2$ is the vaporization rate. Even for the case of non-unity Lewis numbers, the species and energy conservation equations can be combined linearly to obtain transport equations in which the chemical terms do not appear explictly, as shown in earlier work by

Liñán *et al.* (1994). For the droplet-burning problem, linear combinations of the species and energy equations lead to

$$\frac{\dot{m}L_m}{4\pi}\frac{\mathrm{d}Z}{\mathrm{d}r} = \frac{\mathrm{d}}{\mathrm{d}r}\left(\rho_L D_T r^2 \frac{\mathrm{d}\tilde{Z}}{\mathrm{d}r}\right), \tag{2.2}$$

$$\frac{\dot{m}}{4\pi}\frac{\mathrm{d}H}{\mathrm{d}r} = \frac{\mathrm{d}}{\mathrm{d}r}\left(\rho_L D_T r^2 \frac{\mathrm{d}H}{\mathrm{d}r}\right) + \frac{(1-L_{\mathrm{F}})\dot{m}}{4\pi}\frac{\mathrm{d}Y_{\mathrm{F},L}}{\mathrm{d}r} + \frac{(1-L_{\mathrm{O}_2})\dot{m}}{4\pi}\frac{\mathrm{d}\hat{Y}_{\mathrm{O}_2,L}}{\mathrm{d}r}, \tag{2.3}$$

$$\frac{\dot{m}L_{\mathrm{P}}}{4\pi}\frac{\mathrm{d}Y}{\mathrm{d}r} = \frac{\mathrm{d}}{\mathrm{d}r}\left(\rho_L D_T r^2 \frac{\mathrm{d}Y}{\mathrm{d}r}\right) + \frac{(L_{\mathrm{P}}-L_{\mathrm{F}})\dot{m}}{4\pi}\frac{\mathrm{d}Y_{\mathrm{F},L}}{\mathrm{d}r} + \frac{(L_{\mathrm{P}}-L_{\mathrm{O}_2})\dot{m}}{4\pi}\frac{\mathrm{d}\hat{Y}_{\mathrm{O}_2,L}}{\mathrm{d}r}, \tag{2.4}$$

where ρ, c_p, D_T and T are, respectively, the gas density, specific heat at constant pressure, thermal diffusivity and temperature. In this formulation Y_i and $L_i = D_T/D_i$ are, respectively, the mass fraction and Lewis number of species i. The specific heat and Lewis numbers are considered constant in this analysis. The oxidizer and product local mass fractions, $\hat{Y}_{\mathrm{O}_2,L} = Y_{\mathrm{O}_2,L}/Y_{\mathrm{O}_2}$ and $\hat{Y}_{\mathrm{P},L} = Y_{\mathrm{P},L}(1+S_L)/(1+s)$, have been normalized, respectively, with the oxidizer mass fraction far from the droplet and with the product mass fraction generated in a diffusion flame with unity Lewis numbers of the reactants. In the formulation, $L_m = L_{\mathrm{O}_2}(1+S_L)/(1+\tilde{S}_L)$ is a mean Lewis number, with $\tilde{S}_L = S_L L_{\mathrm{O}_2}/L_{\mathrm{F}}$. Additionally, Z and $\tilde{Z}$ are mixture-fraction variables defined as

$$Z = \frac{S_L Y_{\mathrm{F},L} - \hat{Y}_{\mathrm{O}_2,L} + 1}{1+S_L} \quad \text{and} \quad \tilde{Z} = \frac{\tilde{S}_L Y_{\mathrm{F},L} - \hat{Y}_{\mathrm{O}_2,L} + 1}{1+\tilde{S}_L}, \tag{2.5}$$

and H is an excess enthalpy given by

$$H = Y_{\mathrm{F},L} + \hat{Y}_{\mathrm{O}_2,L} + \frac{c_p(T_L - T)}{p_1 q} - 1, \tag{2.6}$$

with $p_1 = L_m/[L_{\mathrm{O}_2}L_{\mathrm{F}}(1+S)]$ a constant. In equation (2.4), the potential product generation

$$Y = Y_{\mathrm{F},L} + \hat{Y}_{\mathrm{O}_2,L} + \frac{\hat{Y}_{\mathrm{P},L} - \hat{Y}_{\mathrm{P}}}{p_2 L_{\mathrm{P}}} - 1 \tag{2.7}$$

is used, with $\hat{Y}_{\mathrm{P}}$ the normalized product mass fraction far from the droplet, and p_2 a second constant given by $p_2 = p_1/Z_{st,L}$. The local density ρ_L is obtained from the equation of state $\rho_L T_L = \rho T$ if negligible changes in the mean molecular weight occur during vaporization and combustion.

Note that the subindex $_L$ is employed in this microscale formulation to denote local magnitudes in the droplet vicinity, hence differentiating them from the mesoscale magnitudes treated below for spray formulations. Therefore, S_L is in general not equal to the global stoichiometric ratio $S = s/Y_{\mathrm{O}_2,\mathrm{A}}$ based on the oxidizer mass fraction of the air feed stream $Y_{\mathrm{O}_2,\mathrm{A}}$ in figure 1. However, far away from the droplet, $Y_{i,L}$, T_L, and $D_{T,L}$ correspond, in the mesoscale formulation, to the mass fractions Y_i, temperature T, and thermal diffusivity D_T of the gas at the droplet location, as depicted in figure 1(c,d). In these variables, the local thermal conductivity and thermal diffusivity vary with the temperature, respectively, as $\kappa_L/\kappa = \hat{\kappa}[T_L/T]$ and $D_{T,L}/D_T = \hat{D}_T[T_L/T]$, which are related as $\hat{D}_T = T_L\hat{\kappa}/T$ for constant specific heat.

Equations (2.1)-(2.4) are subject to the boundary conditions

$$\dot{m}L_v + \dot{q}_d = 4\pi\rho_L D_{T,L} c_p a^2 \frac{\mathrm{d}T}{\mathrm{d}r}, \quad \dot{m}L_m(Z-1) = 4\pi\rho_L D_{T,L} a^2 \frac{\mathrm{d}\tilde{Z}}{\mathrm{d}r},$$
$$\dot{m}H - 4\pi\rho_L D_{T,L} a^2 \frac{\mathrm{d}H}{\mathrm{d}r} = -\frac{\{\dot{m}\,[c_p(T-T_d)+L_v]+\dot{q}_d\}}{p_1 q}$$
$$+(1-L_{\mathrm{F}})\dot{m}(Y_{\mathrm{F},L}-1) + (1-L_{\mathrm{O}_2})\dot{m}\hat{Y}_{\mathrm{O}_2,L}$$

and

$$\dot{m}L_{\mathrm{P}}Y - 4\pi\rho_L D_{T,L} a^2 \frac{\mathrm{d}Y}{\mathrm{d}r} = -\frac{\dot{m}\hat{Y}_{\mathrm{P}}}{p_2} + (L_{\mathrm{P}}-L_{\mathrm{F}})\dot{m}(Y_{\mathrm{F},L}-1)$$
$$+(L_{\mathrm{P}}-L_{\mathrm{O}_2})\dot{m}\hat{Y}_{\mathrm{O}_2,L} \tag{2.8}$$

at $r=a$, and

$$Z=0, \quad \tilde{Z}=0, \quad H=0 \quad \text{and} \quad Y=0 \tag{2.9}$$

at $r\to\infty$.

A uniform temperature T_d is assumed inside the fuel droplet, a good approximation if the heating time scale is much longer than the heat-conduction time a^2/D_{Td} in the droplet, with D_{Td} the thermal diffusivity of the liquid fuel. The heating flux and vaporization rate can be expressed in the form

$$\dot{m} = 4\pi\kappa a\lambda_{v,r}/c_p \quad \text{and} \quad \dot{q}_d = 4\pi\kappa a T Q, \tag{2.10}$$

where the subindices $_v$ and $_r$ refer to the non-reacting and reacting cases respectively. The coefficients λ and Q depend on the ratio of the mesoscale temperature to the droplet temperature T/T_d. The description of these two quantities is simplified for fuels of practical interest, for which $L_v/R_{\mathrm{F}}T_B$ is typically a large number, with R_{F} and T_B representing the fuel gas constant and boiling temperature, respectively. Under those conditions, it is seen that the mass fraction of vapor at the droplet surface is exponentially small during an initial heat-up period corresponding to $T_d < T_B$, in which all the thermal power transferred from the gas is dedicated to increasing the temperature of the yet non-vaporizing droplet. This heat-up period finishes when the liquid temperature reaches values close to the boiling temperature, $(T_d-T_B)/T_B \sim R_{\mathrm{F}}T_B/L_v \ll 1$, and vaporization starts with values of the vapor mass fraction of order unity at the droplet surface. In this vaporizing period the droplet temperature remains equal to the boiling temperature, $T_d = T_B$.

2.1. *Droplet heating and vaporization without chemical reaction*

In the absence of chemical reaction, equation (2.1) may be integrated once with the boundary condition $T=T_d$ at $r=a$ to give

$$\lambda_v(\Theta-\Theta_d) = \eta^2\hat{\kappa}(\Theta)\frac{\mathrm{d}\Theta}{\mathrm{d}\eta} - Q - \lambda_v\ell_v\Theta_B, \tag{2.11}$$

by using the dimensionless variables $\Theta = T_L/T$ and $\eta = r/a$, with λ_v and Q defined in (2.10), and $\Theta_d = T_d/T$. In this formulation, $\ell_v = L_v/c_pT_B$ and $\Theta_B = T_B/T$ are, respectively, the dimensionless latent heat and boiling temperature. The resulting non-reacting problem is thus independent of the fuel and oxidizer Lewis numbers.

The integration of (2.24) is facilitated by introduction of the alternative coordinate x defined from

$$\frac{\hat{\kappa}(\Theta)}{b}\frac{\mathrm{d}x}{x^2} = \frac{\mathrm{d}\eta}{\eta^2}, \tag{2.12}$$

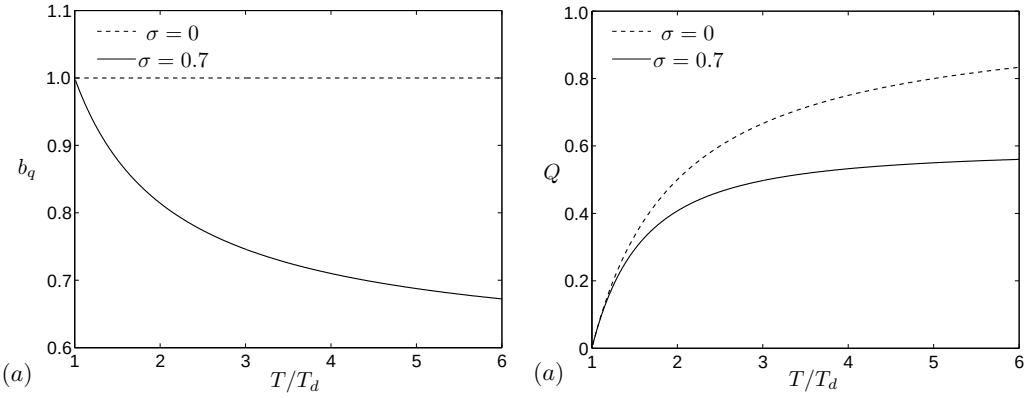

FIGURE 2. (a) The coefficient b_q in (2.15) and (b) the dimensionless heating rate Q in (2.16), as a function of the ratio of dimensionless temperatures T/T_d, and for the power-law $\hat{\kappa} = (T_L/T)^\sigma$.

which reduces the problem to that of integrating the constant-conductivity problem

$$\tilde{\lambda}_v(\Theta - \Theta_d) = x^2 \frac{\mathrm{d}\Theta}{\mathrm{d}x} - \tilde{Q} - \tilde{\lambda}_v \ell_v \Theta_B, \tag{2.13}$$

with $\Theta = \Theta_d$ at $x = 1$, and $\Theta = 1$ at $x \to \infty$. In writing (2.13) the definitions $\tilde{\lambda}_v = \lambda_v/b$ and $\tilde{Q} = Q/b$ have been used. The unknown value of the coefficient b is determined from the condition that $x = 1$ at $\eta = 1$, and can be therefore computed from (2.13) as

$$b = \int_1^\infty \frac{\hat{\kappa}(x)}{x^2} \mathrm{d}x \tag{2.14}$$

once the temperature profile $\Theta(x)$ is obtained.

For $T_d < T_B$, integration of (2.11) with the boundary condition at $x \to \infty$ gives $\Theta = 1 - \tilde{Q}/x$ which in turn determines $\tilde{Q} = 1 - \Theta_d$ when the boundary value $\Theta = \Theta_d$ is imposed at $x = 1$. Using this result in performing the integral (2.14) yields

$$b_q\,(T/T_d, \hat{\kappa}) = \frac{1}{1 - \Theta_d} \int_0^{1-\Theta_d} \hat{\kappa}[1 - w] dw, \tag{2.15}$$

with w a dummy variable of integration. The dimensionless heating rate $Q = b_q \tilde{Q}$, can be finally written as

$$Q = b_q(1 - T_d/T) \tag{2.16}$$

in terms of the temperatures T and T_d of the gas and liquid phases. The variations of the coefficient b_q and the heating rate Q are shown in figure 2 for the power law $\hat{\kappa} = (T_L/T)^\sigma$, for which (2.15) becomes $b_q = (1 - (T_d/T)^{\sigma+1})/[(1 + \sigma)(1 - T_d/T)]$. For $\sigma > 0$ and a given temperature ratio T/T_d, the dimensionless droplet-heating rate Q is smaller than in the case $\sigma = 0$ because of the decrease in the thermal conductivity near the droplet surface.

Vaporization occurs as the droplet reaches a temperature close to the boiling value, $T_d = T_B$. In this stage, $\dot{q}_d = 0$ and integration of (2.13) with the boundary condition at $x \to \infty$ gives

$$\Theta = \Theta_B(1 - \ell_v) + [1 - \Theta_B(1 - \ell_v)] \exp(-\tilde{\lambda}_v/x). \tag{2.17}$$

Imposing now the boundary value $\Theta = \Theta_B$ at $x = 1$ provides an equation that can be

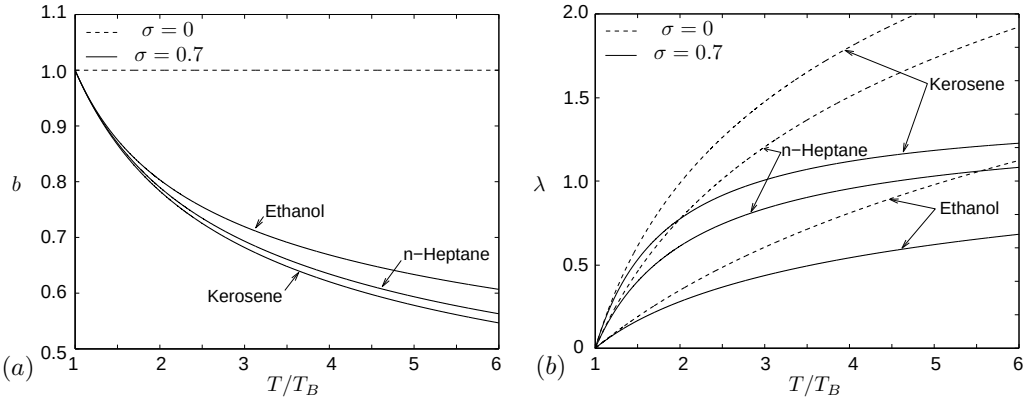

FIGURE 3. (a) Numerical values of the coefficient b_v in (2.19) and (b) the dimensionless vaporization rate λ_v in (2.21), as a function of the ratio of dimensionless temperature θ/θ_B, and for the power-law $\hat{\kappa} = (T_L/T)^{\sigma}$. In this figure, characteristic values of l_v at atmospheric pressure for kerosene ($\ell_v = 0.59$), n-heptane ($\ell_v = 0.85$) and ethanol ($\ell_v = 2.41$) have been used.

solved for $\tilde{\lambda}_v$ to give

$$\tilde{\lambda}_v = \ln\left(1 + \frac{T/T_B - 1}{\ell_v}\right). \tag{2.18}$$

Using now (2.17) and (2.18) in performing the integral (2.14) yields the expression

$$b_v\left(T/T_B, \ell_v, \hat{\kappa}\right) = \frac{1}{\ln\left(1 + \dfrac{T/T_B - 1}{\ell_v}\right)} \int_1^{C_{1v}} \hat{\kappa}\left[1 + \left(1 - \frac{1}{w}\right) C_{2v}\right] \frac{dw}{w} \tag{2.19}$$

for the coefficient b_v as a function of $\hat{\kappa}$, the ratio of the gas temperature to the boiling temperature T/T_B, and the dimensionless latent heat ℓ_v. The constants C_{1v} and C_{2v} are given by

$$C_{1v} = 1 + (T/T_B - 1)/\ell_v \quad \text{and} \quad C_{2v} = (T_B/T)(1 - \ell_v) - 1. \tag{2.20}$$

The variation of b_v with T/T_B and different values of l_v, corresponding to representative fuels, is given in figure 3a. Using this result and the relation $\lambda_v = b_v \tilde{\lambda}_v$, one can finally write the dimensionless vaporization rate as

$$\lambda_v = b_v \ln\left(1 + \frac{T/T_B - 1}{\ell_v}\right) = \int_1^{C_{1v}} \hat{\kappa}\left[1 + \left(1 - \frac{1}{w}\right) C_{2v}\right] \frac{dw}{w}. \tag{2.21}$$

According to (2.19), if the thermal-conductivity variations with the gas temperature are not considered, the coefficient b_v becomes $b_v = 1$ and the dimensionless vaporization rate (2.21) reduces to the well-known Spalding law $\lambda = \ln[1 + c_p(T - T_B)/L_v]$. For $\sigma > 0$, the effective thermal diffusivity in the surroundings of the droplet decreases, and λ_v becomes smaller than the value predicted by the Spalding law as the temperature ratio T/T_B increases, as observed in figure 3b.

2.2. *Droplet burning rate in the Burke-Schumann limit*

During the heating stage, the mass fraction of fuel at the droplet surface is exponentially small and combustion cannot take place. After the heating period, the liquid temperature has reached the boiling point, and a non-negligible amount of fuel vapor is found in the droplet surroundings. If the diffusion time a^2/D_T is larger than the characteristic

chemical time t_{ch}, then the chemical reaction occurs in a diffusion-controlled regime, in which the fuel vapor and the ambient oxidizer react in a thin spherical flame that surrounds the droplet, as depicted in figure 1c. In the Burke-Schumann limit, the fuel and oxidizer regions are separated by an infinitesimally thin flame located at $Z = Z_{st,L} = 1/(1 + S_L)$. This limit is analyzed in what follows for calculating the burning rate λ_r of the fuel droplet.

Using the transformation (2.14), equations (2.2), (2.3) and (2.4) can be written as

$$\tilde{\lambda}_r L_m (Z-1) = x^2 \frac{\mathrm{d}\tilde{Z}}{\mathrm{d}x}, \tag{2.22}$$

$$\tilde{\lambda}_r H = x^2 \frac{\mathrm{d}H}{\mathrm{d}x} + (1-L_{\mathrm{F}})\tilde{\lambda}_r (Y_{\mathrm{F},L}-1) + (1-L_{\mathrm{O}_2})\tilde{\lambda}_r Y_{\mathrm{O}_2,L} - \frac{\tilde{\lambda}_r}{p_1 \tilde{q}}\left[\frac{(1-\Theta_B)}{\Theta_B} + \ell_v\right], \tag{2.23}$$

$$\tilde{\lambda}_r L_{\mathrm{P}} Y = x^2 \frac{\mathrm{d}Y}{\mathrm{d}x} + (L_{\mathrm{P}} - L_{\mathrm{F}})\tilde{\lambda}_r (Y_{\mathrm{F},L}-1) + (L_{\mathrm{P}} - L_{\mathrm{O}_2})\tilde{\lambda}_r Y_{\mathrm{O}_2,L} - \frac{\tilde{\lambda}_r \hat{Y}_{\mathrm{P}}}{p_2}. \tag{2.24}$$

Equations (2.22)-(2.24) are subject to $Z = \tilde{Z} = H = Y = 0$ at $x \to \infty$. In writing (2.24), the temperature of the liquid has been set equal to the boiling temperature, $\tilde{q}_d = 0$ and $T_d = T_B$, since droplet burning occurs after the heating period. In this formulation, $\tilde{q} = q/(c_p T_B)$ is the dimensionless heat of reaction. Inspection of equations (2.22)-(2.24) shows that Z, $\tilde{Z}$ H, Y, $\mathrm{d}\tilde{Z}/\mathrm{d}x$, $\mathrm{d}H/\mathrm{d}x$ and $\mathrm{d}Y/\mathrm{d}x$ are continuous across the flame, but $\mathrm{d}Z/\mathrm{d}x$, $\mathrm{d}^2\tilde{Z}/\mathrm{d}x^2$, $\mathrm{d}^2H/\mathrm{d}x^2$ and $\mathrm{d}^2Y/\mathrm{d}x^2$ are not continuous there unless $L_{\mathrm{O}_2} = L_{\mathrm{F}} = L_{\mathrm{P}} = 1$.

Integration of (2.22)-(2.24) shows that, in the infinitely-fast-chemistry limit, an oxidizer region exists for $Z < Z_{st,L}$ in which

$$\begin{aligned}
\hat{Y}_{\mathrm{O}_2,L} = 1 - \frac{Z}{Z_{st,L}}, \quad Y_{\mathrm{F},L} = 0, \quad \hat{Y}_{\mathrm{P},L} = \hat{Y}_{\mathrm{P}} + p_2 L_{\mathrm{P}} \left(Y + \frac{Z}{Z_{st,L}}\right), \\
\Theta = 1 + \left[1 - \exp(-\tilde{\lambda}_r/x)\right]\left[\Theta_B - 1 + (\tilde{q} - \ell_v)\Theta_B\right], \\
Z = 1 - \mathrm{e}^{-\tilde{\lambda}_r L_{\mathrm{O}_2}/x}, \\
H = \frac{\mathrm{e}^{-\tilde{\lambda}_r L_{\mathrm{O}_2}/x} - \mathrm{e}^{-\tilde{\lambda}_r/x}}{Z_{st,L}} + \left\{(1-L_{\mathrm{O}_2})\left(\frac{1-Z_{st,L}}{Z_{st,L}}\right)\right. \\
\left. + \frac{1}{p_1\tilde{q}}\left[\frac{(1-\Theta_B)}{\Theta_B} + \ell_v\right] + 1 - L_{\mathrm{F}}\right\}\left(\mathrm{e}^{-\tilde{\lambda}_r/x} - 1\right), \\
Y = \frac{\mathrm{e}^{-\tilde{\lambda}_r L_{\mathrm{O}_2}/x} - \mathrm{e}^{-\tilde{\lambda}_r L_{\mathrm{P}}/x}}{Z_{st,L}} + \left\{(L_{\mathrm{P}} - L_{\mathrm{O}_2})\left(\frac{1-Z_{st,L}}{Z_{st,L}}\right)\right. \\
\left. + \frac{\hat{Y}_{\mathrm{P}}}{p_2} + L_{\mathrm{P}} - L_{\mathrm{F}}\right\}\left(\frac{\mathrm{e}^{-\tilde{\lambda}_r L_{\mathrm{P}}/x} - 1}{L_{\mathrm{P}}}\right).
\end{aligned} \tag{2.25}$$

The region (2.25) is separated by a flame surface from a fuel region located on the other

side of the flame, $Z_L > Z_{st,L}$, in which

$$\hat{Y}_{\mathrm{O}_2,L} = 0, \quad Y_{\mathrm{F},L} = \frac{Z - Z_{st,L}}{1 - Z_{st,L}}, \quad \hat{Y}_{\mathrm{P},L} = \hat{Y}_{\mathrm{P}} + p_2 L_{\mathrm{P}} \left(Y + \frac{1 - Z}{1 - Z_{st,L}} \right)$$

$$\Theta = \Theta_B(1 - \ell_v) + \frac{c_H p_1 \Theta_B \tilde{q}}{Z_{st,L}} \exp(-\tilde{\lambda}_r/x),$$

$$Z = 1 - \frac{\mathrm{e}^{-\tilde{\lambda}_r L_{\mathrm{F}}/x}}{(1 - Z_{st,L})^{(L_{\mathrm{F}}/L_{\mathrm{O}_2} - 1)}},$$

$$H = \frac{c_H \mathrm{e}^{-\tilde{\lambda}_r/x}}{Z_{st,L}} - \frac{\mathrm{e}^{-\tilde{\lambda}_r L_{\mathrm{F}}/x}}{(1 - Z_{st,L})^{L_{\mathrm{F}}/L_{\mathrm{O}_2}}} - \frac{1}{p_1 \tilde{q}} \left[\frac{(1 - \Theta_B)}{\Theta_B} + \ell_v \right],$$

$$Y = \frac{c_Y \mathrm{e}^{-\tilde{\lambda}_r L_{\mathrm{P}}/x}}{Z_{st,L} L_{\mathrm{P}}} - \frac{\mathrm{e}^{-\tilde{\lambda}_r L_{\mathrm{F}}/x}}{(1 - Z_{st,L})^{L_{\mathrm{F}}/L_{\mathrm{O}_2}}} - \frac{\hat{Y}_{\mathrm{P}}}{p_2 L_{\mathrm{P}}}. \tag{2.26}$$

The constants of integration

$$c_H = \left[1 - (1 - Z_{st,L})^{-1/L_{\mathrm{O}_2}}\right] \left[(1 - L_{\mathrm{O}_2})(1 - Z_{st,L}) + (1 - L_{\mathrm{F}}) Z_{st,L} - 1\right] + \left[\frac{(1 - \Theta_B)}{\Theta_B} + \ell_v \right] \frac{Z_{st,L}}{p_1 \tilde{q}},$$

$$c_Y = \left[1 - (1 - Z_{st,L})^{-L_{\mathrm{P}}/L_{\mathrm{O}_2}}\right] \Big[(L_{\mathrm{P}} - L_{\mathrm{O}_2})(1 - Z_{st,L}) + (L_{\mathrm{P}} - L_{\mathrm{F}}) Z_{st,L} - L_{\mathrm{P}}\Big] + \frac{Z_{st,L} \hat{Y}_{\mathrm{P}}}{p_2} \tag{2.27}$$

are obtained by matching at the flame position x_f, which is given by

$$x_f = \tilde{\lambda}_r L_{\mathrm{O}_2} \Big/ \ln \left(\frac{1}{1 - Z_{st,L}} \right). \tag{2.28}$$

Equation (2.28) is obtained by evaluating Z at $Z = Z_{st,L}$. Similarly, the equilibrium flame temperature

$$\Theta_f = 1 + \left[1 - (1 - Z_{st,L})^{1/L_{\mathrm{O}_2}}\right] \left[\Theta_B - 1 + (\tilde{q} - \ell_v)\Theta_B\right] \tag{2.29}$$

is obtained by evaluating Θ at $x = x_f$.

The reduced burning rate $\tilde{\lambda}_r$ can be calculated by setting $\Theta = \Theta_B$ in (2.26) at the droplet surface $x = 1$, which gives

$$\tilde{\lambda}_r = \ln \left(1 + \frac{\tilde{q}^\star \tilde{Y}_{\mathrm{O}_2}/S + T/T_B - 1}{\ell_v} \right), \tag{2.30}$$

with $\tilde{q}^\star$ representing a modified heat release per unit mass of oxidizer,

$$\frac{\tilde{q}^\star \tilde{Y}_{\mathrm{O}_2}}{S} = \left[\left(1 + \frac{\tilde{Y}_{\mathrm{O}_2}}{S} \right)^{1/L_{\mathrm{O}_2}} - 1 \right] \tilde{q}. \tag{2.31}$$

In writing (2.30) and (2.31), the substitutions $Z_{st,L} = (\tilde{Y}_{\mathrm{O}_2}/S)/(1 + \tilde{Y}_{\mathrm{O}_2}/S)$ and $L_m = L_{\mathrm{O}_2} L_{\mathrm{F}}(1 + \tilde{Y}_{\mathrm{O}_2}/S)/(L_{\mathrm{O}_2} + L_{\mathrm{F}} \tilde{Y}_{\mathrm{O}_2}/S)$ have been made to express $Z_{st,L}$ and L_m as a function of the local oxidizer mass fraction $\tilde{Y}_{\mathrm{O}_2} = Y_{\mathrm{O}_2}/Y_{\mathrm{O}_2,\mathrm{A}}$ normalized with the oxidizer mass fraction in the air feed stream, as indicated in figure1.

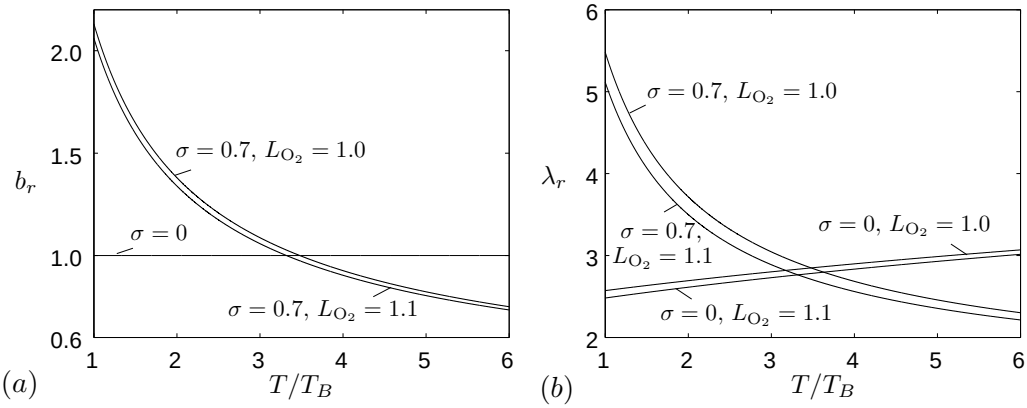

FIGURE 4. (a) Numerical values of the coefficient b_v in (2.32) and (b) the dimensionless vaporization rate λ_v in (2.34), as a function of the ratio of dimensionless temperature T/T_B, and for the power-law $\hat{\kappa} = (T_L/T)^{\sigma}$. In this figure, characteristic values of l_v and $\tilde{q}$ at atmospheric pressure for n-heptane ($\ell_v = 0.85$, $\tilde{q} = 119.9$) have been used, with $S = 14.7$ and $\tilde{Y}_{O_2} = 1.0$.

Using (2.25) and (2.26) in performing the integral (2.14) yields the expression

$$b_r(T/T_B, \tilde{Y}_{O_2}/S, \tilde{q}, \ell_v, L_{O_2}, \hat{\kappa}) = \frac{1}{\ln\left(1 + \dfrac{\tilde{q}^{\star}\tilde{Y}_{O_2}/S + T/T_B - 1}{\ell_v}\right)}$$
$$\times\left\{ \int_1^{C_{4r}} \hat{\kappa}\left[1 + \left(1 - \frac{1}{w}\right) C_{2r}\right] \frac{dw}{w} + \int_{C_{4r}}^{C_{1r}} \hat{\kappa}\left[\frac{C_{3r}}{w} + C_{5r}\right] \frac{dw}{w} \right\}, \qquad (2.32)$$

where C_{ir} are constants given by

$$C_{1r} = 1 + \frac{\tilde{q}^{\star}\tilde{Y}_{O_2}/S + T/T_B - 1}{\ell_v}, \quad C_{2r} = (T_B/T)(1 - \ell_v) - 1 + (T_B/T)\tilde{q},$$
$$C_{3r} = \ell_v (T_B/T) C_{1r}, \quad C_{4r} = \left(1 + \tilde{Y}_{O_2}/S\right)^{1/L_{O_2}}, \quad C_{5r} = (T_B/T)(1 - \ell_v). \qquad (2.33)$$

Using now (2.30), (2.32) and the relation $\lambda_r = b_r \tilde{\lambda}_r$, the dimensionless burning rate can be written as

$$\lambda_r(T/T_B, \tilde{Y}_{O_2}/S, \tilde{q}, \ell_v, L_{O_2}, \hat{\kappa}) = b_r \ln\left(1 + \frac{\tilde{q}^{\star}\tilde{Y}_{O_2}/S + T/T_B - 1}{\ell_v}\right)$$
$$= \left\{ \int_1^{C_{4r}} \hat{\kappa}\left[1 + \left(1 - \frac{1}{w}\right) C_{2r}\right] \frac{dw}{w} + \int_{C_{4r}}^{C_{1r}} \hat{\kappa}\left[\frac{C_{3r}}{w} + C_{5r}\right] \frac{dw}{w} \right\}, \qquad (2.34)$$

with $\tilde{q}^{\star}$ given by (2.31) and the constants C_{ir} calculated from (2.33).

In expression (2.34), an apparent dimensionless temperature $T^{\star}/T_B = T/T_B + \tilde{q}^{\star}\tilde{Y}_{O_2}/S$ plays the role of the vaporization-driving temperature in analogy with the result (2.21) for the droplet-vaporization rate of non-burning droplets. Note that $T^{\star}$ is the effective temperature seen by the burning droplet, as indicated by taking the limit $x \to \infty$ in the gas temperature on the fuel side (2.26). The value of $T^{\star}$ is larger than the temperature of the flame and the surrounding gas, as depicted in figure 1c.

The variations of b_r and λ_r with T/T_B and different values of ℓ_v, $\tilde{q}$ and L_{O_2} are given

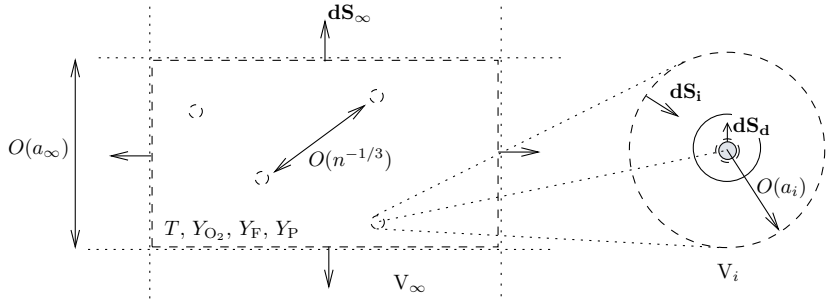

FIGURE 5. Sketch of control volumes used in Section 3.

in figure 4. Note that, according to this formulation, λ_r is independent of L_{F}, since the flame burns all the fuel that arrives by advection in the fast-chemistry limit (Williams 1965). This suggests that, in this model, the droplet-burning rate of fuels such as heptane burning in air, for which $L_{\mathrm{F}} \sim 2.5$ and $L_{\mathrm{O_2}} \sim 1.1$, is only weakly affected by the non-unity Lewis number of the oxidizer. Figure 4b shows a decay of the burning rate for $\sigma > 0$ when a temperature power-law is taken for the thermal conductivity. According to the temperature boundary condition in (2.8) at the droplet surface, the burning rate λ_r is proportional to $(\kappa_B/\kappa)\partial\Theta/\partial\eta$ -where κ_B is the thermal conductivity of the vapor at the boiling temperature-, with the thermal-conductivity ratio κ_B/κ decreasing more rapidly than the rate of increase of the temperature gradient as T/T_B increases. Non-unity oxidizer Lewis numbers and gas thermal-conductivity variations produce shifts in the flame position, in that the flame is pushed outwards as $L_{\mathrm{O_2}}$ increases above unity. Variable thermal conductivity effects $\sigma > 0$ bring the flame closer to the droplet surface.

The formulas derived above reduce to well-known results for burning droplets with unity-Lewis numbers of fuel and oxidizer, $L_{\mathrm{O_2}} = L_{\mathrm{F}} = 1$, for which the flame is located at $x_f = \tilde{\lambda}_r/\ln(1+\tilde{Y}_{\mathrm{O_2}}/S)$ with a dimensional equilibrium temperature $T_f = T + (\tilde{Y}_{\mathrm{O_2}}/S)[T_B - T + (q - L_v)/c_p]/(1+\tilde{Y}_{\mathrm{O_2}}/S)$ and, since $\tilde{q}^\star = \tilde{q}$ in this equidiffusive limit, the droplet burning rate becomes $\lambda_r = b_r \ln[1 + (q\tilde{Y}_{\mathrm{O_2}}/S + c_pT - c_pT_B))/L_v]$ (Williams 1965). Note also that (2.30) and (2.34) are, respectively, equal to the vaporization results (2.19) and (2.21) for zero heat release $\tilde{q} = 0$, which are independent of L_{F} and $L_{\mathrm{O_2}}$.

3. Derivation of fuel-spray source-terms for the mesoscale conservation equations

In this section, the spray source-terms in the mass, momentum, species and energy conservation equations for the gas-phase are derived from integral analysis based on the results provided in the previous section. The analysis uses a Lagrangian framework for illustration.

Consider a volume V_i bounded by a sphere S_i of radius a_i, with $a_i/a \gg 1$, as depicted in figure 5. The surface S_i envelops the droplet and moves with it at a velocity $\mathbf{v}_d$. In this region, droplet heating, vaporization and burning are described, in the limit of small Péclet numbers $\mathrm{Pe}_d \ll 1/S_L \ll 1$, by equations (2.1)-(2.6). The surrounding temperature and mass fractions in the gas are, respectively, T, Y_{F}, $Y_{\mathrm{O_2}}$ and Y_{P}. In order to preserve the quasi-steady dynamics described by equations (2.1)-(2.4), the radius a_i is assumed to be sufficiently large such that the characteristic diffusion time at radial distances of $O(a_i)$ is larger than the vaporization time scale, or equivalently, that $a_i/a > (\rho_d/\rho)^{1/2}$.

Additionally, a_i is taken to be much smaller than the droplet interspace, $na_i^3 \ll 1$, for neglecting droplet-droplet interactions. Similarly, if the droplet is burning, the flame radius needs to be located within S_i, with $a_i/a_f \gg 1$. The radius a_i is also assumed to be much smaller than the smallest of the aerodynamic spatial scales, in such a way that momentum, energy and composition gradients need to vary in scales which are large compared to a_i. Therefore, in numerical applications the computational cell size may be larger than a_i, and the droplet radius may be much smaller than the Kolmogorov scale for the point-source Lagrangian treatment of the vaporizing droplets to remain accurate.

Finite Péclet-number effects produced by droplet inertia tend to push the flame radially inwards and lead to diffusion-flame extinction. Therefore, the single-droplet combustion regime depicted in figure 1c may exist only for sufficiently slow sprays. Fundamental studies addressing finite Péclet-number effects on the microscale dynamics of vaporizing and burning droplets have been performed in earlier works (Hermanns 2006; Del Álamo & Williams 2007), but the resulting analytical framework is complex and has not yet been implemented in numerical calculations of sprays, which typically make use of experimental correlations for calculating the source terms (Sirignano 1999).

Consider now a larger stationary volume V_∞ that contains the droplet and the surface S_i, and which is bounded by a closed surface S_∞ of characteristic size a_∞, with $a_\infty = O(1/n^{1/3})$, as depicted in figure 5. Gaseous flames may exist within V_∞ if, for instance, the vaporization Stokes number of the spray is large. In the example depicted in figure 1, a case of particular interest for analyzing heterogeneous combustion effects is that in which the droplet lifetime is much longer than the flow time based on the local strain rate. In that example, the counterflow diffusion-flame thickness δ_f is of $O(\Delta_f^{-1/3}/\beta)$ in scales of order δ_M, as indicated by a reaction-diffusion balance, with $\Delta_f \sim \delta_M^2/(D_T t_{chf}) \gtrsim O(1)$ and $\beta \gg 1$ the Damköhler and Zel'dovich numbers, respectively. Since the thickness of the droplet diffusion flame δ_d is of $O(\Delta_d^{-1/3}/\beta)$ in scales of $O(a)$, with $\Delta_d \sim a^2/(D_T t_{chd})$ the droplet Damköhler number, it is concluded that $\delta_d/\delta_f \sim a/\delta_M$ for $\Delta_d/\Delta_f = O(1)$. For sprays with $a/\delta_M \ll 1$, which correspond to sprays with Stokes numbers $\mathrm{St} = (\rho_d/\rho)(a/\delta_M)^2 \ll \rho_d/\rho$, the thickness of the droplet diffusion flame is much smaller than the thickness of the counterflow diffusion flame, $\delta_d/\delta_f \ll 1$. Smaller Stokes numbers $\mathrm{St} \ll (\rho_d/\rho)\beta^{-2}\Delta_f^{-2/3}$ are needed for the droplet radius to be smaller than the counterflow diffusion-flame thickness, $a/\delta_f \ll 1$. Furthermore, if the quasi-steady results (2.21) and (2.34) are used for spherically symmetric point-source approximations of droplets near flames, even smaller values of the Stokes number $\mathrm{St} \ll \beta^{-2}\Delta_f^{-2/3}$ should be taken for avoiding partial intrusion of the reaction zone in the surrounding volume V_i.

In the limit $na_i^3 \ll 1$, in which $\mathrm{S}_i/\mathrm{S}_\infty \to 0$, the Gauss theorem can be used to derive the differential conservation equations for the gas phase from their integral forms in the volume V_∞, which gives

$$\frac{\partial \rho}{\partial t} + \nabla \cdot (\rho \mathbf{v}) = \sum_{j=1}^{N} \frac{\delta(\mathbf{x} - \mathbf{x_j})}{V_\infty} \phi_{\rho,j}, \tag{3.1}$$

$$\frac{\partial}{\partial t}(\rho \mathbf{v}) + \nabla \cdot (\rho \mathbf{v}\mathbf{v}) = \nabla \cdot \overline{\overline{\tau}} + \sum_{j=1}^{N} \frac{\delta(\mathbf{x} - \mathbf{x_j})}{V_\infty} \phi_{v,j}, \tag{3.2}$$

$$\frac{\partial}{\partial t}(\rho \Gamma_k) + \nabla \cdot (\rho \Gamma_k \mathbf{v}) = -\nabla \cdot \mathbf{F}_\mathbf{k}'' + R_k + \sum_{j=1}^{N} \frac{\delta(\mathbf{x} - \mathbf{x_j})}{V_\infty} \phi_{k,j}, \tag{3.3}$$

with $\mathbf{x_j}$ the droplet position, $\overline{\overline{\tau}}$ the stress tensor, δ the Dirac-delta function and N the number of droplets. In this formulation, $\Gamma_k = \{\tilde{Y}_{\mathrm{O}_2}, Y_{\mathrm{F}}, \tilde{Y}_{\mathrm{P}}, c_pT\}$ are the transported scalars, $\mathbf{F''_k} = \{\mathbf{J''}_{\mathrm{O}_2}, \mathbf{J''}_{\mathrm{F}}, \mathbf{J''}_{\mathrm{P}}, \mathbf{q''}\}$ are the diffusion fluxes of mass and energy, and $R_k = \{-S\omega_{\mathrm{F}}, -\omega_{\mathrm{F}}, (1+S)\omega_F, q\omega_F\}$ are the corresponding chemical source terms, with $\tilde{Y}_{\mathrm{O}_2} = Y_{\mathrm{O}_2}/Y_{\mathrm{O}_2,A}$ the mass fraction of oxidizer normalized with the oxidizer mass fraction in the feed stream, $\tilde{Y}_{\mathrm{P}} = Y_{\mathrm{P}}(1+S)/(1+s)$ the normalized mass fraction of combustion products, $\mathbf{J}''_i = -(\rho D_T/L_i)\nabla Y_i$ the mass-diffusion fluxes, $\mathbf{q''} = -\rho c_p D_T \nabla T$ the heat-diffusion flux, ω_F the mass of fuel consumed per unit time and unit volume by chemical conversion, q the chemical heat release, and $S = s/Y_{\mathrm{O}_2,A}$ the mesoscale stoichiometric coefficient. In this formulation, $\phi_{k,j}$ are the source terms induced by the heating, vaporization and combustion of a single droplet, which can be obtained by calculating the mass, momentum and energy fluxes on S_i from the results given in the previous section,

$$\phi_{\rho,j} = -\int_{\mathrm{S}_i} \rho(\mathbf{v}-\mathbf{v_d})\cdot\mathbf{dS} = \begin{cases} 0 \quad \text{(Heating)} \\ 4\pi a\kappa\lambda_v/c_p \quad \text{(Vaporization)} \\ 4\pi a\kappa\lambda_r/c_p \quad \text{(Burning)} \end{cases} \tag{3.4}$$

$$\phi_{m,j} = -\int_{\mathrm{S}_i} \rho\mathbf{v}(\mathbf{v}-\mathbf{v_d})\cdot\mathbf{dS} + \int_{\mathrm{S}_i} \overline{\overline{\tau}}\cdot\mathbf{dS}$$

$$= \begin{cases} 6\pi\mu a(\mathbf{v_d}-\mathbf{v}) \quad \text{(Heating)} \\ 6\pi\mu a(\mathbf{v_d}-\mathbf{v}) + 4\pi a\kappa\lambda_v\mathbf{v_d}/c_p \quad \text{(Vaporization)} \\ 6\pi\mu a(\mathbf{v_d}-\mathbf{v}) + 4\pi a\kappa\lambda_r\mathbf{v_d}/c_p \quad \text{(Burning)} \end{cases} \tag{3.5}$$

$$\phi_{\mathrm{F},j} = -\int_{\mathrm{S}_i} \rho Y_{\mathrm{F},L}(\mathbf{v}-\mathbf{v_d})\cdot\mathbf{dS} - \int_{\mathrm{S}_i} \mathbf{J}''_{\mathrm{F}}\cdot\mathbf{dS} = \begin{cases} 0 \quad \text{(Heating)} \\ 4\pi a\kappa\lambda_v/c_p \quad \text{(Vaporization)} \\ 0 \quad \text{(Burning)} \end{cases} \tag{3.6}$$

$$\phi_{\mathrm{O}_2,j} = -\int_{\mathrm{S}_i} \rho\tilde{Y}_{\mathrm{O}_2,L}(\mathbf{v}-\mathbf{v_d})\cdot\mathbf{dS} - \int_{\mathrm{S}_i} \mathbf{J}''_{\mathrm{O}_2}\cdot\mathbf{dS} = \begin{cases} 0 \quad \text{(Heating)} \\ 0 \quad \text{(Vaporization)} \\ -4\pi a\kappa\lambda_r S/c_p \quad \text{(Burning)} \end{cases} \tag{3.7}$$

$$\phi_{\mathrm{P}} = -\int_{\mathrm{S}_i} \rho\tilde{Y}_{\mathrm{P},L}(\mathbf{v}-\mathbf{v_d})\cdot\mathbf{dS} - \int_{\mathrm{S}_i} \mathbf{J}''_{\mathrm{P}}\cdot\mathbf{dS} = \begin{cases} 0 \quad \text{(Heating)} \\ 0 \quad \text{(Vaporization)} \\ 4\pi a\kappa\lambda_r(1+S)/c_p \quad \text{(Burning)} \end{cases} \tag{3.8}$$

$$\phi_T = -\int_{\mathrm{S}_i} \rho c_p T_L(\mathbf{v}-\mathbf{v_d})\cdot\mathbf{dS} - \int_{\mathrm{S}_i} \mathbf{q}''\cdot\mathbf{dS}$$

$$= \begin{cases} -4\pi a\kappa TQ \quad \text{(Heating)} \\ 4\pi a\kappa\lambda_v(c_pT_B - L_v)/c_p \quad \text{(Vaporization)} \\ 4\pi a\kappa\lambda_r(c_pT_B + q - L_v)/c_p \quad \text{(Burning)} \end{cases} \tag{3.9}$$

where Q, λ_v and λ_r are given in equations (2.16), (2.21) and (2.34), respectively.

4. Conclusions

In this study, expressions for simplified calculations were derived for the droplet heating, vaporization and combustion rates for fuel droplets in gases with non-unity Lewis numbers and temperature-dependent thermal conductivities. The resulting formulas (2.16), (2.21) and (2.34), which were computed in figures 2, 3 and 4, were expressed in terms of the local gas variables in mesoscopic scales. Additionally, source terms were calculated for

heating, vaporizing and burning sprays in the single-droplet combustion regime. However, a criterion for selection between vaporizing and burning source terms has not been provided here since the droplet-flame interaction dynamics and the droplet ignition problem have not been addressed.

A number of limitations are germane to the quasi-steady spherically-symmetric point-source treatments of fuel droplets, many of which have been outlined above. Additionally, it is found in liquid-fueled combustors that the Kolmogorov length is often of the same order as the droplet radius, and therefore the Kolmogorov turnover time becomes of the same order as the diffusion time around the droplet. In this limit, the droplet heating, vaporization and combustion processes lose spherical symmetry and become unsteady. Similar limitations arise in droplet-flame interactions in fuel sprays, for which the strong thermal gradients in the gas at droplet-interspacing scales may render unphysical any continuum treatment of the liquid phase. Further research on the microscale physics of droplet phenomena in turbulent flows is needed to address these points.

Acknowledgments

Support from NASA, grant #NNX07AC72A, is acknowledged.

REFERENCES

Del Álamo, G. & Williams, F. A. 2007 Theory of vaporization of a rigid spherical droplet in slowly varying rectilinear flow at low Reynolds number. *J. Fluid Mech.* **580**, 219–249.

Hermanns, M. 2006 *High-order numerical methods applied to the analysis of transport phenomena in combustion.* Ph.D. Thesis, Departamento de Motopropulsión y Termofluidodinámica, Escuela Superior de Ingenieros Aeronáuticos, Universidad Politécnica de Madrid.

Li, S. 1997 Spray stagnation flames. *Prog. Energy Combust. Sci.* **23**, 303–347.

Liñán, A., Orlandi, P., Verzicco, R. & Higuera, F. J. 1994 Effects of non-unity Lewis numbers in diffusion flames. *Proceedings of the Summer Program*, Center for Turbulence Research, NASA Ames/Stanford University pp. 5–18.

Luo, K., Pitsch, H., Pai, M. G. & Desjardins, O. 2011 Direct numerical simulations and analysis of three-dimensional n-heptane spray flames in a model swirl combustor. *Proc. Combust. Inst.* **33**, 2143–2152.

Sirignano, W. 1999 *Fluid dynamics and transport of droplets and sprays.* Cambridge University Press.

Williams, F. A. 1965 *Combustion Theory.* Addison-Wesley.